Power Mean Based Image Segmentation in the Presence of Noise

Afzal Rahman
University of Peshawar
Haider Ali
University of Peshawar
Noor Badshah
University of Engineering and Technology Peshawar
Muhammad Zakarya
Abdul Wali Khan University
Hameed Hussain
University of Buner
Izaz Ur Rahman
Abdul Wali Khan University
Aftab Ahmed
Abdul Wali Khan University
Muhammad Haleem (m.haleem@kardan.edu.af)
Kardan University

Research Article

Keywords: noise and outliers, image segmentation, variational framework, intensity inhomogeneity, art models

Posted Date: January 11th, 2022

DOI: https://doi.org/10.21203/rs.3.rs-1204261/v1

Power mean based image segmentation in the presence of noise

Afzal Rahman[1], Haider Ali[1], Noor Badshah[2,+], Muhammad Zakarya[3,+], Hameed Hussain[4], Izaz Ur Rahman[3,+], Aftab Ahmed[3], and Muhammad Haleem[5,+,*]

[1]Department of Mathematics, University of Peshawar, Pakistan
[2]Department of Basic Sciences, University of Engineering and Technology Peshawar, Pakistan
[3]Department of Computer Science, Abdul Wali Khan University, Mardan, Pakistan
[4]Department of Computer Science, University of Buner, Pakistan
[5]Department of Computer Science, Kardan University, Kabul, Afghanistan
[*]m.haleem@kardan.edu.af
[+]these authors contributed equally to this work

ABSTRACT

In image segmentation and in general in image processing, noise and outliers distort contained information posing in this way a great challenge for accurate image segmentation results. To ensure a correct image segmentation in presence of noise and outliers, it is necessary to identify the outliers and isolate them during a denoising pre-processing or impose suitable constraints into a segmentation framework. In this paper, we impose suitable removing outliers constraints supported by a well-designed theory in a variational framework for accurate image segmentation. We investigate a novel approach based on the power mean function equipped with a well established theoretical base. The power mean function has the capability to distinguishes between true image pixels and outliers and, therefore, is robust against outliers. To deploy the novel image data term and to guaranteed unique segmentation results, a fuzzy-membership function is employed in the proposed energy functional. Based on qualitative and quantitative extensive analysis on various standard data sets, it has been observed that the proposed model works well in images having multi-objects with high noise and in images with intensity inhomogeneity in contrast with the latest and state of the art models.

1 Introduction

Image segmentation is a fundamental step in computer vision and in digital image processing. The main idea of image segmentation is to visualize meaningful objects in a given scene or image[1,2] linked to many important fields such as medical imaging, object detection, video, traffic control systems, surveillance, automated surgeries, and so on[3–5]. Several different approaches for image segmentation exist including clustering[3], thresholding[6], edge detection and region-based models[7–10], Markov random fields[7,8], stochastic methods[9,10], etc. However, images are diverse in nature, and frequently happens that one model working for a particular class or type of images may not properly work for other types. Some well-known factors which normally affect the performance of the segmentation models are noise and outliers, intensity inhomogeneity and low contrast between background and foreground in a given image[4,11]. To cope with these issues, achieving accurate image segmentation, the active contour framework is a very popular technique due to the flexibility of allowing the impose of desired constraints. Moreover, the availability of robust implementations, such as efficient optimization, and fast numerical methods is crucial. The main idea in active contour methods[1,7–10,12–17] is to allow dynamical curves to move autonomously on a given image which locates boundaries of the objects/regions therein. The active contour models mainly use the concept of variational calculus[1,21–25], that is functional optimization. It can be easily observed that the variational models for image processing in general and for segmentation, in particular, derive an energy functional which is minimized to get the desired results. The active contour models can be mainly divided into three categories, region-based[1,12–16,18], edge-based models[7–10] and region and edge based models[26]. A milestone variational model for segmentation purposes introduced by Mumford-Shah (MS)[1] aims to obtain a smooth cartoon image that leads to edge detection. It is important to note that the design of the MS model is for ideal images, that is,

images without noise, outliers and intensity inhomogeneity. Moreover, the direct implementation of this model is not feasible[22]. To easily implement the MS model, the Chan *et al.* (CV)[9] restricted the MS model to a piecewise function reconstruction (two phases). By phase here we mean the set of homogeneous intensity pixels which can be easily distinguished from other sets of homogeneous intensity pixels in a given image. We should emphasize that the CV model ignores the presence of noise and other factors such as intensity inhomogeneity[23]. This fact can be easily observed from the fitting data term used in CV model

$$\int_{\text{inside}(\Gamma)} |\mathbf{u}(x,y)-c_1|^2 dxdy + \int_{\text{outside}(\Gamma)} |\mathbf{u}(x,y)-c_2|^2 dxdy, \tag{1}$$

where $\mathbf{u}(x,y)$ is the given image with $(x,y) \in \Omega$ a rectangular domain, c_1, c_2 are constants and Γ denotes boundary of the objects. In discrete sense, this data term is based on the least square based objective function

$$\frac{1}{|\,\Omega\,|}\sum_{i,j}(\mathbf{u}(i,j)-\mathbf{c})^2, \tag{2}$$

whose minimum is the sample mean $\mathbf{c} = (c_1, c_2) = \bar{\mathbf{x}}$ inside and outside Γ. From the formula, easily can be observed that the sample mean is affected by outliers. To improve CV model, many techniques has been introduced in the last decades. In contrast with CV model, Li *et al.*[38] proposed the Local Binary Fitting (LBF) model which performs much better and resembles more with the MS model by carrying out the segmentation via approximating given image with two locally smooth functions. Although, this model tackles intensity inhomogeneity but not noise. This phenomenon is can be observed by analysing the data fitting term

$$\int_{\Omega} K_\sigma * |\mathbf{u}(x,y)-c_1|^2 dxdy + \int_{\Omega} K_\sigma * |\mathbf{u}(x,y)-c_2|^2 dxdy, \tag{3}$$

where K_σ is Gaussian kernel. In a discrete and local sense this data term is also based on the least square based objective function

$$\sum_{N_x}(\mathbf{u}(i,j)-\mathbf{c})^2, \tag{4}$$

in local neighborhood N_x whose minimum is also the sample mean $\mathbf{c} = \bar{\mathbf{x}}$. In other words, the LBF model uses the concept of the CV model but in local neighborhoods throughout image domain Ω. This leads to wider image intensity variation in small patches but on the other hand, it is more prone to noise and outliers as compared to the CV model. In this way, the fitting term takes into account the image intensity variance in small patches but on the other hand, it is more prone to noise and outliers as compared to the CV model. Moreover, this model is not convex so consequently one need tune several times the position of initial guess for the desired results. Mondal *et al.*[16] introduced a new model based on a trade-off local and global information. The model shows good performance for images with intensity inhomogeneity and presence of noise and outliers. The experimental results shown in different data sets indicate that the model can deal with intensity inhomogeneity images, blurred boundary or discontinuous edges, and presence of moderated noise. Chuang *et al.*[19] and Tripathy *et al.*[20] introduced the models which work better for the noisy MRI images, but may not work well for the images with intensity inhomogeneity. This model is not convex so consequently one need tune several times the position of initial guess for the desired results. Recently, Wu *et al.*[24] proposed a convex variational segmentation model based on the concept of coefficient of variation (CoV) by ignoring the factor and presence of noise and outliers in given images. This argument is validated by the fact that their CoV based image data fitting term is sum of squares divided by sum of image intensity. Similar to the average fitting term in the CV model the value of the average fitting term in the Wu *et al.*[24] model shows sensitivity to noise and outliers[27]. To further improve this model, Wu *et al.*[12] proposed an active contour model incorporating a kernel metric, which is robust, stable, and works well for images with low noise and outliers. Ali et al.[28] introduced Lehmer's type generalized mean

$$\frac{\sum_{i,j}\mathbf{u}(i,j)^p}{\sum_{i,j}\mathbf{u}(i,j)^{p-1}}, \tag{5}$$

in an segmentation framework, where p is any real number. Although this average is very effective in multi-region segmentation and suitable to different image intensity backgrounds it requires further analysis to tackle noise and outliers.

The above discussion summarises that most of the variational region-based image segmentation models are based on the least square function which forces the fit of the data to a piecewise function of the mean intensity values of the foreground and background. This is the main reason that the aforementioned models and similar are unable to correctly segment noisy and outliers affected images[28].

In this article, we mainly focus to design an efficient image data fitting term based on a novel objective function

$$\left(\frac{1}{|\,\Omega\,|}\sum_{i,j}(||\mathbf{u}(i,j)-a||_2^2)^p\right)^{\frac{1}{p}}. \tag{6}$$

As further will be explained in Section 3 this term is robust against the outliers by giving very fewer weights to outliers and noise in contrast with the traditional and old objective function which gives equal or almost equal weights to outliers and true image pixels[29].Moreover, besides the new data fitting term of the proposed model, a fuzzy level set function is employed which has two main benefits over the traditional level set function. Firstly, a single fuzzy function can capture more than one phase or objects of different intensities at the same time[30,31]. Secondly, it plays an important role in efficiently imposing constraints for implementing convexity. This lead to non-dependence of the initial guess. Furthermore, for a deeper understanding of the proposed model, the mathematical analysis is presented. For the regularization of the fuzzy membership function, the Gaussian smoothing filtering is employed. Following are the major contributions of this work:

- we impose suitable removing outliers constraints supported by a well-designed theory in a variational framework for accurate image segmentation;
- we investigate a novel approach based on the power mean function equipped with a well established theoretical base;
- to guarantee unique segmentation results, a fuzzy-membership function is employed in the proposed energy functional; and
- extensive analysis on various standard data sets, it has been observed that the proposed model works well in images having multi-objects with high noise.

The rest of the paper is organized as follows. In Section 2, we give a brief review of related segmentation models. The design and analysis of the proposed novel model are presented in Section 3. In Section 4, a comprehensive experimental analysis is carried out both qualitative and quantitatively for types of outdoor natural, synthetic and medical images compared to existing and latest state-of-the-art segmentation techniques. Final remarks and conclusions are made in Section 5.

2 Related works

2.1 Active contours without edges (CV)

To easily implement the MS model[1], Chan *et al.* (CV)[9] restricted the MS model to a piecewise function reconstruction (two phases). Chan *et al.*[9] consider a piecewise constant function which divides the image into different homogeneous regions representing the foreground and background. For the image $\mathbf{u}$, the minimization energy functional is given by:

$$\begin{aligned} F^{CV}(a_1,a_2,\Gamma) = {} & \mu\ length(\Gamma) \\ & + \lambda_1 \int_{inside(\Gamma)} |\mathbf{u}(x,y)-c_1|^2 dxdy \\ & + \lambda_2 \int_{outside(\Gamma)} |\mathbf{u}(x,y)-c_2|^2 dxdy, \end{aligned} \tag{7}$$

where $\lambda_1,\ \lambda_2,\ \mu \geq 0$ are constants which tune the weight between the smoothing and the fitting terms. Γ is the contour, and c_1, c_2 are average intensities of given image $I_0(x,y)$ for foreground and background respectively. This is a non convex model, so consequently one need to tune several times the position of initial guess for the desired results.

2.2 Fuzzy energy-based minimization (FEBM)

Given an image, $\mathbf{u}(x,y)$ in a spacial domain Ω Krinidis et al.[31] proposed a segmentation model based on fuzzy function embedded in active contour variational framework:

$$\begin{aligned} &F(\Gamma, c_1, c_2, v) = \mu length(\Gamma) \\ &+ \eta_1 \int_{\Omega} [\mathbf{z}(x,y)]^m |\mathbf{u}(x,y) - c_1|^2 dxdy \\ &+ \eta_2 \int_{\Omega} [1 - \mathbf{z}(x,y)]^m |\mathbf{u}(x,y) - c_2|^2 dxdy \end{aligned} \tag{8}$$

where the constants c_1, c_2 stand for average values inside and outside the contour Γ, respectively, m is the weight exponent (normally taking the value 2), $\eta_1, \eta_2 > 0$ and $\mu \geq 0$ are constants. The function $\mathbf{z}(x,y) \in [0,1]$ is the fuzzy membership function representing the membership degree of $\mathbf{u}(x,y)$ inside the Γ and $1 - \mathbf{z}(x,y)$ is the membership degree of $\mathbf{u}(x,y)$ outside the Γ. For a fast convergence of the minimization problem in Eq. (8) the authors use a fast algorithm as proposed by Song and Chan[32]. This model can segment images with multi-objects, different intensity variations objects, and hazy boundaries, however, it may not properly segment noisy images. The reason is that this model uses the same conventional least square objective function which fits the data to the mean value of the foreground and background.

2.3 A convex variational level set model for image segmentation (CVMS)

Wu *et al.*[24] proposed a strictly convex functional for two-phase image segmentation:

$$\begin{aligned} F_{WH}(\psi) = \eta &\int_{\Omega} \frac{(\mathbf{u}(x,y) - c_1)^2}{{c_1}^2} (\psi(x,y) + 1)^2 dxdy \\ &+ \int_{\Omega} \frac{(\mathbf{u}(x,y) - c_2)^2}{{c_2}^2} (\psi(x,y) - 1)^2 dxdy \end{aligned} \tag{9}$$

where ψ denote the level set function[5], $\eta > 0$ is a parameter. Eq. (9) is strictly convex, and it is flexible to its initial contour place, but it may not work for the noisy images as we can see in Fig. 2 and Fig. 3. In the theoretical aspect, the image data fitting term in a discrete sense is based on the concept of squared CoV, $CoV^2 = \sum_{i,j} \frac{(\mathbf{u}(i,j) - \mathbf{a})^2}{\mathbf{a}^2}$ whose minimum turns out to be $\mathbf{a} = \frac{\sum_{i,j} \mathbf{u}(i,j)^2}{\sum_{i,j} \mathbf{u}(i,j)}$. The value of this average and the objective function both are sensitive to noise and outliers[27] similar to CV model. That is the main reason why the Wu model is unable to work in noisy images and performs worst than the CV model.

2.4 Fuzzy active contour (FAC) model

In contrast with the traditional L_2 norm fidelity term based models, a fuzzy active contour model with kernel metric is proposed by Wu *et al.*[12], which is based on the following fuzzy function:

$$\begin{aligned} &F(\Gamma, c_1, c_2, z) = \mu length(\Gamma) \\ &+ \eta_1 \int_{\Omega} [\mathbf{z}(x,y)]^m (1 - \hat{k}(\mathbf{u}(x,y), c_1)) dxdy \\ &+ \eta_2 \int_{\Omega} [1 - \mathbf{z}(x,y)]^m (1 - \hat{k}(\mathbf{u}(x,y), c_2)) dxdy, \end{aligned} \tag{10}$$

where the kernel metric $\hat{k}(\xi_1, \xi_2) = \langle \chi(\xi_1), \chi(\xi_2) \rangle$ and given ξ_1, ξ_2 vectors and $\chi(.)$ a nonlinear map. Here $\langle \chi(\xi_1), \chi(\xi_2) \rangle$ is the inner product of $\chi(\xi_1)$ and $\chi(\xi_2)$. Gaussian radial basis function $\hat{k}(\xi_1, \xi_2)$ is given by:

$$\hat{k}(\xi_1, \xi_2) = \exp\left(-\frac{(\xi_1 - \xi_2)^2}{\rho} \right) \tag{11}$$

where ρ is the parameter. From Figs. 2-7 in the experimental section it is clear that Eq. (10) may not work for noisy images although $\hat{k}$ serves as a weight function which is supposed to assign suitable weights to image true pixel and outliers. In the model implementation, the outliers get enough weights to affect the segmentation performance of this model in noisy images.

2.5 Unconditional stable method for bimodal (USMB) image segmentation

Li *et al.*[15], proposed the the following energy functional which is based on Lee *et al.*[33] idea of e a stationary global minimum:

$$\begin{aligned} & F(c_1, c_2, \psi) \\ &= \eta_1 \int_\Omega (\mathbf{u}(x,y) - c_1)^2 \psi(x,y) H(1 + \psi(x,y)) dxdy \\ &- \eta_2 \int_\Omega (\mathbf{u}(x,y) - c_2)^2 \psi(x,y) H(1 - \psi(x,y)) dxdy, \end{aligned} \tag{12}$$

with H the Heaviside function and c_1, c_2 constants.

Li *et al.*[15] showed that for any time step the proposed scheme is unconditionally stable. Moreover, with the assumption that $|\psi^n| \leq 1$ it is easy to show that $|\psi^{n+1}| \leq 1$, which leads to a straightforward update of ψ^{n+1} from given ψ^n. Although the method shows stability for image segmentation of synthetic and real images with moderated noise the method, similar to the above ideas were the least square fit directs to the mean of the foreground and background, shows sensitivity to high noise and outliers[29].

Ali et al.[34] introduced Lehmer's type generalized mean in an segmentation framework. Although this average is very effective in multi-region segmentation and suitable to different image intensity backgrounds it requires further analysis to tackle noise and outliers. Goldstein *et al.*[37] used Bregman-split method which is well known for its speed, but may not work very well for images with intensity inhomogeneous. Furat *et al*[39] proposed Techniques for the Segmentation of Tomographic Image Data of Functional Materials by combining machine learning methods and conventional image processing steps. This approach produced good segmentation results specially for tomographic images.

3 Proposed model

As mentioned above, most of the active contour region-based variational segmentation models consider ideal image while constructing the energy functionals. This can be very easily observed by investigating the utilized image statistical information incorporated in objective functions, such as averages, the measure of dispersions, variance and standard deviation. In literature most of the variational region-based image segmentation models are based on the CV model fitting term idea which is sensitive to noise and outliers[29], or similar to the work in[24,26] which is very robust and effective when detecting edges and boundaries of low contrast but very sensitive when there is noise and outliers[27].

To improve the state of the art models mentioned in related works, we propose a new method which incorporates the power mean into the robust discrete objective function by replacing the traditional models where the arithmetic mean has been used. To handle a noisy image one can design a formulation in the continuous framework based on averages and measure of dispersions. Furthermore, the employment of a fuzzy membership function has its advantages over the traditional level set function as allows the evolve of less number of functions to capture many objects of different intensities[30,31].

Initially, we discuss the power mean function and its property of canceling the negative effect of outliers. We continue in the second subsection with the presentation of the proposed model guided by a fuzzy function based formulation. The rest of the section analyses the convexity of the energy functional, its semi-continuity and coercivity.

3.1 Power mean

Definition. For a given gray scale image $\mathbf{u}(x,y) \in \Omega$ of size $N \times M$, power mean can be defined in discrete form as follows[29,34]:

$$M_p(\mathbf{I}) = \left(\frac{1}{NM} \sum_{i=1,j=1}^{N,M} \mathbf{u}(i,j)^p \right)^{\frac{1}{p}}, \tag{13}$$

where $p \neq 0$, and $\mathbf{u}(i,j) > 0$ is the intensity value at a certain pixel (i,j). For different value of p, such as $p = 1, 0, -1$, the general mean represents specific mean variations such as arithmetic, geometric or harmonic mean.

The parameter p controls the contribution of each sample's element by handling each of them differently according to their the significance. Oh et al.[29] and Ali et al.[34] has been introduced an implementation of such feature. They expressed the general power mean as a linear combination of the elements in the set and

its simplification form as:

$$\sum_{i=1,j=1}^{N,M} \mathbf{u}(i,j)^p = \sum_{i=1,j=1}^{N,M} y(i,j)\mathbf{u}(i,j), \tag{14}$$
$$y(i,j) = \mathbf{u}(i,j)^{p-1}, \text{ for } i = 1,2,...,N \text{ and } j = 1,2,...,M.$$

The employment of the generalized mean controls the a trade-off between the negativeness of outliers in the observed set. It is easy to observe that, the generalized mean in Eq. (14) is an arithmetic mean if $p = 1$. The weight $y(i,j)$ decreases (increases) as $\mathbf{u}(i,j)$ increases (decreases) if $p \leq 1$. This indicates that Eq. (14) is more affected by the small intensity values in the given image $\{\mathbf{u}(i,j)\}_{i=1,j=1}^{N,M}$ and if p decreases, the extent of the affectedness increases. In[35], this information played a key role in applying the generalized mean approach. To develop the ancient models, Oh et. al[29] exchange the conventional least square sample mean fitting term with the generalized mean fitting term as below:

$$m_G(\mathbf{I}) = \arg\min_{\mathbf{a}} \left(\frac{1}{NM} \sum_{i=1,j=1}^{N,M} \left(||\mathbf{u}(i,j) - \mathbf{a}||_2^2 \right)^p \right)^{\frac{1}{p}}, \tag{15}$$

where $\mathbf{a}$ is any arbitrary value in a given image intensity values. We observe that Eq. (15) converts to the traditional CV objective function for $p = 1$ which is based on the conventional arithmetic mean of the squared distance[29,34]. One can choose $p < 1$[29,34] to reduce the negative effects of outliers. In such a way, as p decreases the contribution of a large number to the objective function decreases. Further, Eq. (15) can be written as[29,34]:

$$m_G(\mathbf{I}) = \arg\min_{\mathbf{a}} \sum_{i=1,j=1}^{N,M} \left(||\mathbf{u}(i,j) - \mathbf{a}||_2^2 \right)^p. \tag{16}$$

The basic condition for the generalized sample mean m_G to be a local minimum of the objective function (15) is that the gradient of this function with respect to $\mathbf{a}$ is equal to zero[29,34], that is

$$\frac{\partial}{\partial \mathbf{a}} \left(\sum_{i=1,j=1}^{N,M} \left(||\mathbf{u}(i,j) - \mathbf{a}||_2^2 \right)^p \right) = 0. \tag{17}$$

Similar to the expectation-maximization algorithm scheme, Oh et al.[29] develop an iterative form for easily solvig Eq. (16). First, rewriting Eq. (16) in the form of Eq. (14) and then approximated by a quadratic function

$$||\mathbf{u}(i,j) - \mathbf{a}||_2^2$$

which can be optimized as:

$$\sum_{i=1,j=1}^{N,M} \left(||\mathbf{u}(i,j) - \mathbf{a}||_2^2 \right)^p \approx \sum_{i=1,j=1}^{N,M} \beta(i,j)^{(k)} ||\mathbf{u}(i,j) - \mathbf{a}||_2^2 \tag{18}$$

where

$$\beta^{(k)}(i,j) = \left(||\mathbf{u}(i,j) - \mathbf{a}^{(k)}||_2^2 \right)^{p-1}, \tag{19}$$

for k number of the iterations. The approximation is exact when $\mathbf{a} = \mathbf{a}^{(k)}$. Here, $\mathbf{a}^{(k)}$ can be updated based on the computed $\beta(i,j)$ in Eq. (18). The approximated function based on computed $\beta(i,j)$ is:

$$\frac{\partial}{\partial \mathbf{a}} \beta^{(k)}(i,j) ||\mathbf{u}(i,j) - \mathbf{a}||_2^2 = 0. \tag{20}$$

Then, as a weighted average of the samples $\mathbf{a}^{(k+1)}$ can be computed by (19) and it gives:

$$\mathbf{a}^{(k+1)} = \frac{1}{\sum_{i=1,j=1}^{N,M} \beta^{(k)}(i,j)} \left(\sum_{i=1,j=1}^{N,M} \beta^{(k)}(i,j)\mathbf{u}(i,j) \right). \tag{21}$$

It is important to point out that the function β serves as a weight function that assigns suitable weights to the true image pixels and outliers[29,34]. The parameter p controls the function β and its optimal tuning value has been shown to be in the range $0.6 \leq p \leq 0.8$[29,34]. In the following, we show a new implementation of generalized mean in fuzzy membership variational segmentation framework, which has been fully studied in the work of Oh et al.[29].

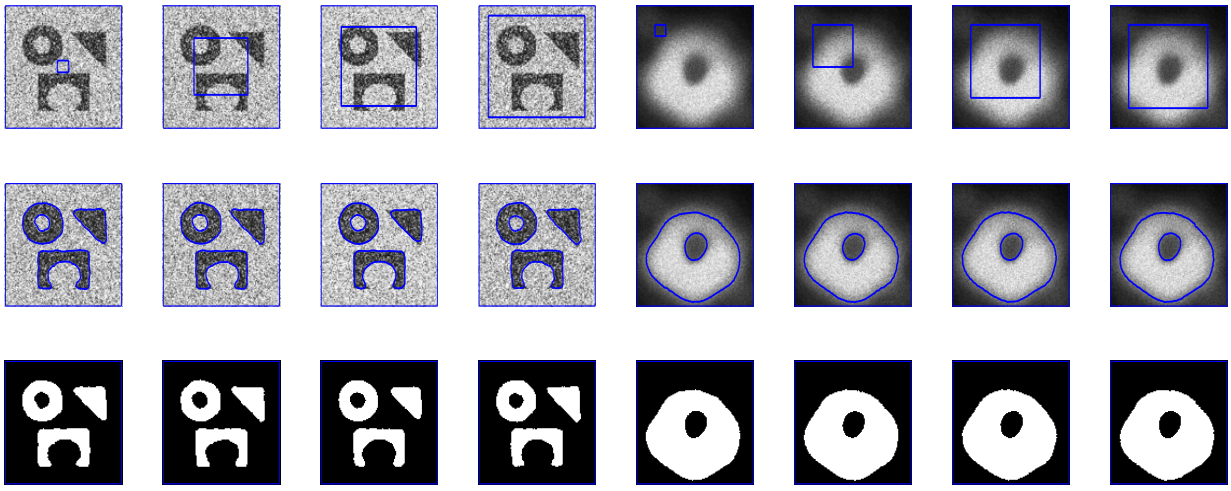

Figure 1. Illustration of the proposed segmentation method for the first ever black hole image and noisy images taken from[31,36] papers. First row: different initial contours. Second row: final contours. Third row: segmented results with $p = 0.5$, μ=0.7, and σ=3 .

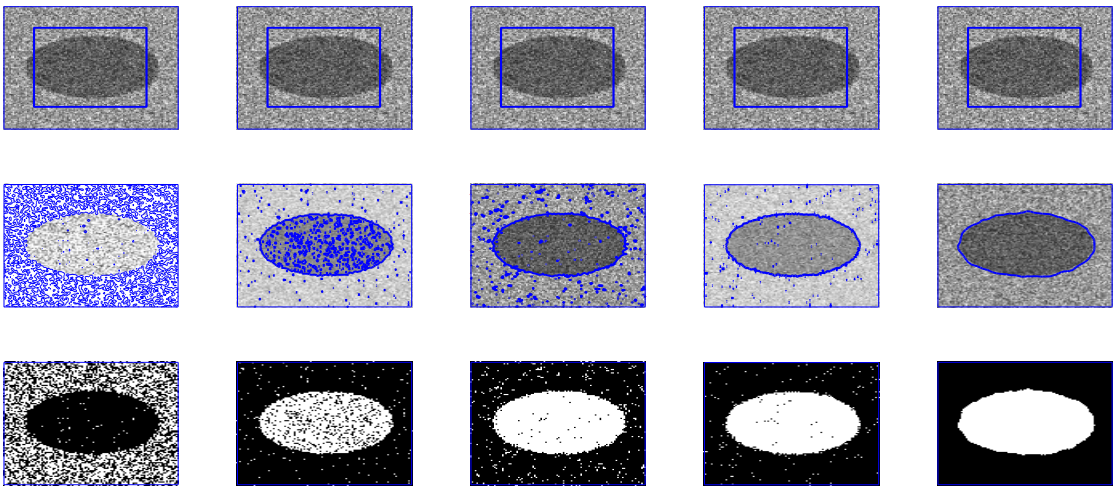

Figure 2. This image is taken from Berkeley's data set. First row shows the given image and the zero level set initialization, the second row shows the segmentation contour and the last row the binary image resulting from the reconstruction of each method involved in the comparison. First, second, third and fourth coulumns are the segmentation results of Wu *et al.*[24], Li *et al.*[15], Wu *et al.*[12] and Krinidis *et al.*[31], respectively. Fifth coulumn illustrates the result of proposed model with $p = 0.5$, μ=0.7, σ=3, with speckle noise = 0.2.

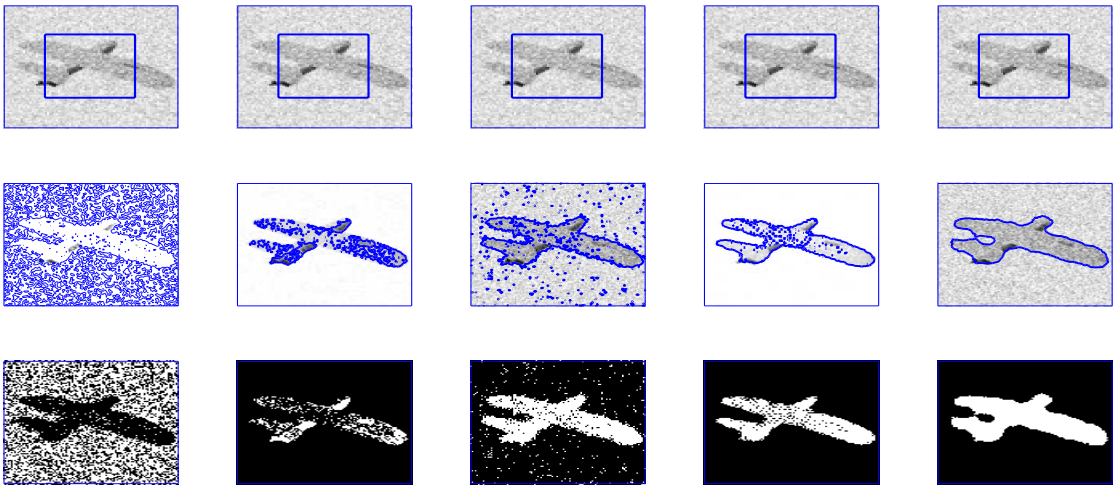

Figure 3. First row shows the given image and the zero level set initialization, the second row shows the segmentation contour and the last row the binary image resulting from the reconstruction of each method involved in the comparison. First, second, third and fourth coulumns are the segmentation results of Wu *et al.*[24], Li *et al.*[15], Wu *et al.*[12] and Krinidis *et al.*[31], respectively. Fifth coulumn illustrates the result of proposed model with $p = 0.5$, μ=0.7, σ=3, with speckle noise = 0.2.

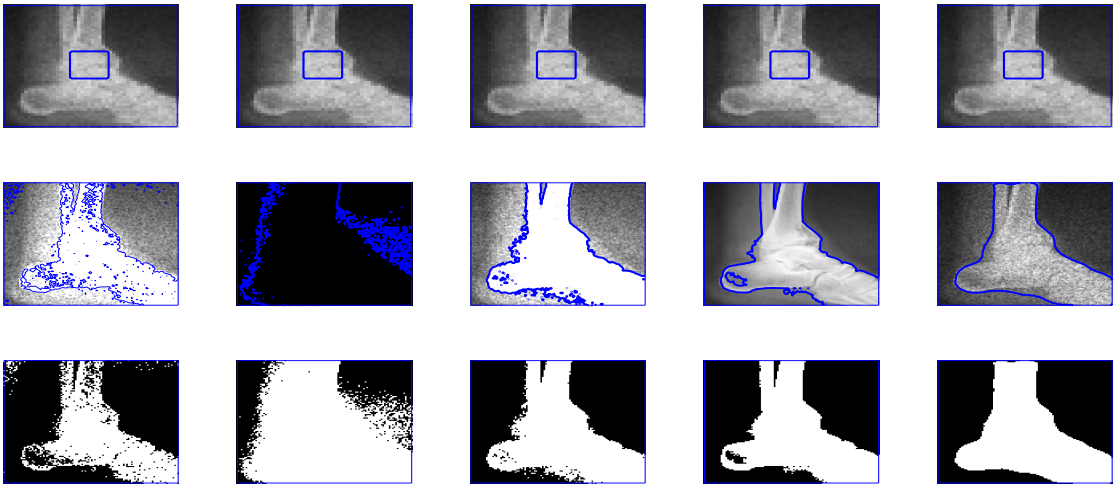

Figure 4. First, second, third and fourth coulumns are the segmentation results of Wu *et al.*[24], Li *et al.*[15], Wu *et al.*[12] and Krinidis *et al.*[31], respectively. Fifth column is the segmentation result of proposed model with p=0.6, μ=0.7, σ=3, and noise = 0.1.

3.2 A new fuzzy function segmentation model led by data-guided outliers avoidance

Defining the image $\mathbf{u}$ on $\Omega \subset \Re^2$, and $\Omega_i \subseteq \Omega$ are disjoint connected open subsets with a piecewise smooth boundary C ($\cup_i \Omega_i$). $\{C_i \in \Re^2|_{i=1}^n\}$ are the curves of the samples to be segmented and $\{c_i \in \Re^2|_{i=1}^n\}$ are their homogeneous associated means. The task of image segmentation is to divide an image into n group of data samples $\{C_i|_{i=1}^n\}$. To improve the segmentation accuracy in the presence of outliers we investigate a novel approach where the quality of generalized sample mean is taken into account and incorporated as a fitting term in a minimization functional. Concretely, we use the Euclidean distance of an input sample C_i to representative samples c_i by allowing in this way some pixels of C_i to be recognized as outliers. In this case, the c_i value not necessary must be near to these samples which consequently brings robustness to outliers. Based on this simple idea we modify the Chan-Vese active contour model in the following form:

$$\begin{aligned} & F(c_1,c_2,C) = \mu length(C) \\ + & \left(\frac{1}{N_1(C)}\int_{inside(C)}(\|\mathbf{u}(x,y)-c_1\|_2^2 dxdy)^p\right)^{\frac{1}{p}} \\ + & \left(\frac{1}{N_2(C)}\int_{outside(C)}(\|\mathbf{u}(x,y)-c_2\|_2^2 dxdy)^p\right)^{\frac{1}{p}}, \end{aligned} \tag{22}$$

here we have three terms, first on is the curve length term, the second and third terms, which we will further refer as $F_1(C)$ and $F_2(C)$, are the new fitting-terms with $N_1(C)$ and $N_2(C)$ the number of points inside and outside the curve C, respectively. By the same argument as we get Eq. (16):

$$F_1(C) = \int_{inside(C)}(\|\mathbf{u}(x,y)-c_1\|_2^2 dxdy)^p, \tag{23}$$

$$F_2(C) = \int_{outside(C)}(\|\mathbf{u}(x,y)-c_2\|_2^2 dxdy)^p, \tag{24}$$

and by the same way to Eq. (18), we get:

$$F_1(C) \approx \int_{inside(C)}\alpha(x,y)\|\mathbf{u}(x,y)-c_1\|_2^2 dxdy, \tag{25}$$

$$F_2(C) \approx \int_{outside(C)}\beta(x,y)\|\mathbf{u}(x,y)-c_2\|_2^2 dxdy, \tag{26}$$

where

$$\alpha(x,y) = (\|\mathbf{u}(x,y)-c_1\|_2^2)^{p-1}, \tag{27}$$

and

$$\beta(x,y) = (\|\mathbf{u}(x,y)-c_2\|_2^2)^{p-1}. \tag{28}$$

Incorporating the fuzzy membership function $\mathbf{z}(x,y)$, Eq. (16) can be rewritten as:

$$\begin{aligned} \int_{z>0.5} & \alpha(x,y) \quad \|\mathbf{u}(x,y)-c_1\|_2^2 dxdy \\ & = \int_\Omega \alpha(x,y)\|\mathbf{u}(x,y)-c_1\|_2^2[\mathbf{z}(x,y)]^m dxdy, \end{aligned} \tag{29}$$

and

$$\begin{aligned} \int_{z<0.5} & \beta(x,y)\|\mathbf{u}(x,y)-c_2\|_2^2 dxdy \\ & = \int_\Omega \beta(x,y)\|\mathbf{u}(x,y)-c_2\|_2^2[1-\mathbf{z}(x,y)]^m dxdy, \end{aligned} \tag{30}$$

where α, β are updated through c_1 and c_2 in each step using Eq. (27), (28) and $\mathbf{z}$ is the fuzzy membership function. We propose the following minimization functional:

$$\begin{aligned} & F(\mathbf{z},c_1,c_2) = \mu\int_\Omega |\nabla \mathbf{z}(x,y)|dxdy \\ & + \int_\Omega \alpha(x,y)\|\mathbf{u}(x,y)-c_1\|_2^2[\mathbf{z}(x,y)]^m dxdy \\ & + \int_\Omega \beta(x,y)\|\mathbf{u}(x,y)-c_2\|_2^2[1-\mathbf{z}(x,y)]^m dxdy. \end{aligned} \tag{31}$$

Keeping c_1 and c_2 fixed in Eq. (31), then minimizing $F(\mathbf{z}, c_1, c_2)$ with respect to $\mathbf{z}$, we get the associated Euler-Lagrange equation for $\mathbf{z}$, t is an artificial time parameterizing the descent direction as:

$$\begin{aligned}\frac{\partial \mathbf{z}}{\partial t} &= \mu\nabla\Big(\frac{\nabla \mathbf{z}}{|\nabla \mathbf{z}|}\Big)\\ &- m\alpha(x,y)[\mathbf{z}(x,y)]^{m-1}\|\mathbf{u}(x,y)-c_1\|_2^2\\ &+ m\beta(x,y)[1-\mathbf{z}(x,y)]^{m-1}\|\mathbf{u}(x,y)-c_2\|_2^2 = 0\\ &\text{in} \quad (0,\infty)\times\Omega,\end{aligned} \tag{32}$$

with

$$\begin{aligned}&\mathbf{z}(0,x,y) = \mathbf{z}(x,y) \quad \text{in} \quad \Omega\\ &\frac{\mathbf{z}}{|\nabla \mathbf{z}|}\frac{\partial \mathbf{z}}{\partial \overrightarrow{n}} \quad \text{on} \quad \partial\Omega,\end{aligned} \tag{33}$$

where $\overrightarrow{n}$ is the normal to the boundary $\partial\Omega$ in exterior, $\alpha(x,y)$ is defined in Eq. (27), $\beta(x,y)$ is defined in Eq. (28) and $\frac{\partial \mathbf{z}}{\partial \overrightarrow{n}}$ is the normal derivative of $\mathbf{z}$ at $\partial\Omega$.

It is important to note that c_1 and c_2 are updated through α and β in each step using Eq. (21).

$$c_1 = \frac{1}{\int_\Omega \alpha(x,y)[\mathbf{z}(x,y)]^m}\int_\Omega \alpha(x,y)\mathbf{u}(x,y)[\mathbf{z}(x,y)]^m, \tag{34}$$

$$c_2 = \frac{1}{\int_\Omega \beta(x,y)[1-\mathbf{z}(x,y)]^m}\int_\Omega \beta(x,y)\mathbf{u}(x,y)[1-\mathbf{z}(x,y)]^m. \tag{35}$$

Keeping c_1, c_2 fixed and $\mu = 0$, then minimizing the energy functional (30) with respect to the fuzzy membership function $\mathbf{z}$, as in[31] we get:

$$z = \frac{1}{1+\Big(\frac{\alpha(x,y)||\mathbf{u}(x,y)-c_1||_2^2}{\beta(x,y)||\mathbf{u}(x,y)-c_2||_2^2}\Big)^{\frac{1}{m-1}}}. \tag{36}$$

Moreover, this updated value is used in the numerical explicit solution of the following Euler Lagrange's equation

$$\begin{aligned}\frac{\partial \mathbf{z}(x,y)}{\partial t} &= \mu\nabla\frac{\nabla \mathbf{z}(x,y)}{|\nabla \mathbf{z}(x,y)|}\\ &+ m[\mathbf{z}(x,y)]^{m-1}||\mathbf{u}(x,y)-c_1||_2^2\\ &+ m[1-\mathbf{z}(x,y)]^{m-1}||\mathbf{u}(x,y)-c_2||_2^2.\end{aligned} \tag{37}$$

Introduction a time step Δt the above equation can be solved with the time marching method as following:

$$\begin{aligned}z^{k+1}(x,y) &= z^k(x,y)+\Delta t\Big[\mu\nabla\frac{\nabla \mathbf{z}(x,y)}{|\nabla \mathbf{z}(x,y)|}\\ &+ m[\mathbf{z}(x,y)]^{m-1}||\mathbf{u}(x,y)-c_1||_2^2\\ &+ m[1-\mathbf{z}(x,y)]^{m-1}||\mathbf{u}(x,y)-c_2||_2^2\Big].\end{aligned} \tag{38}$$

The principal steps of the proposed model are shown in the following algorithm form:

In the following we explore some mathematical properties related to the convexity of the proposed functional (30) which are important to obtain the global minimum.

3.3 Convexity of the energy functional

For simplicity, consider the energy functional in Eq. (31) as follow:

$$f(\zeta) = \mu f_1(\zeta) + f_2(\zeta) + f_3(\zeta) \tag{39}$$

where $\zeta = (x, y)$,

$$f_1(\zeta) = \int_\Omega |\bigtriangledown \mathbf{z}(\zeta)| d\zeta, \tag{40}$$

$$f_2(\zeta) = \int_\Omega \alpha(\zeta)||\mathbf{u}(\zeta) - c_1||_2^2 [\mathbf{z}(\zeta)]^m d\zeta, \tag{41}$$

$$f_3(\zeta) = \int_\Omega \beta(\zeta)||\mathbf{u}(\zeta) - c_2||_2^2 [1 - \mathbf{z}(\zeta)]^m d\zeta. \tag{42}$$

First of all, the domain Ω is convex, because it is a rectangle. The function $f_1(\zeta)$ is convex as in[25]. Consider

$$f_2(\zeta) = \int_\Omega \alpha(\zeta)||\mathbf{u}(\zeta) - c_1||_2^2 [\mathbf{z}(\zeta)]^m d\zeta. \tag{43}$$

Taking $F_2(\zeta) = \alpha(\zeta)||\mathbf{u}(\zeta) - c_1||_2^2 [\mathbf{z}(\zeta)]^m$, where $F_2 : \Omega \to R$ such that

$$f_2(\zeta) = \int_\Omega F_2(\zeta) d\zeta. \tag{44}$$

Let $\zeta_1 = (x_1, y_1), \zeta_2 = (x_2, y_2) \in \Omega$ and $\kappa \in [0, 1]$, since Ω is convex, we can write:

$$\begin{aligned} \kappa\zeta_1 + (1-\kappa)\zeta_2 &= (\kappa(x_1, y_1) + (1-\kappa)(x_2, y_2)) \\ &= (\kappa(x_1 - x_2) + x_2, \kappa(y_1 - y_2) + y_2) \in \Omega. \end{aligned} \tag{45}$$

Taking the derivative of $F_2(\zeta)$ with respect to the function $\mathbf{z}(\zeta)$, we get

$$\frac{\partial F_2}{\partial \mathbf{z}} = m[\mathbf{z}(\zeta)]^{m-1} \alpha(\zeta)||\mathbf{u}(\zeta) - c_1||_2^2. \tag{46}$$

Differentiating again with respect to $\mathbf{z}(\zeta)$, we get

$$\frac{\partial^2 F_2}{\partial \mathbf{z}^2} = m(m-1)[\mathbf{z}(\zeta)]^{m-2} \alpha(x, y)||\mathbf{u}(\zeta) - c_1||_2^2. \tag{47}$$

$\frac{\partial^2 F_2}{\partial \mathbf{z}^2} \geq 0$, as $\mathbf{z}(\zeta) \in [0, 1]$, $m = 2$, $\alpha(\zeta) \geq 0$ and $||\mathbf{u} - c_1||_2^2 \geq 0$, also Ω is convex. Thus $F_2(\zeta)$ is convex and for all $\zeta_1, \zeta_2 \in \Omega$ and $\kappa \in [0, 1]$ the inequality

$$F_2(\kappa\zeta_1 + (1-\kappa)\zeta_2) \leq \kappa F_2(\zeta_1) + (1-\kappa) F_2(\zeta_2) \tag{48}$$

holds. From Eq. (48), we have

$$\begin{aligned} &\int_\Omega F_2(\kappa\zeta_1 + (1-\kappa)\zeta_2) d\zeta \\ &\qquad \leq \kappa \int_\Omega F_2(\zeta_1) d\zeta + (1-\kappa) \int_\Omega F_2(\zeta_2) d\zeta. \end{aligned} \tag{49}$$

Using Eq. (39), we get

$$f_2(\kappa\zeta_1 + (1-\kappa)\zeta_2) \leq \kappa f_2(\zeta_1) + (1-\kappa) f_2(\zeta_2), \tag{50}$$

which means that f_2 is convex. In the same way, one can prove the convexity of f_3. Thus $f(\zeta)$ is convex with respect to $\mathbf{z}(\zeta)$ being the sum of convex functions.

3.4 Lower semi-continuity and coercivity

Theorem 1. For the energy functional Eq. (31) and for fixed α, β, c_1, c_2, there exists at least one solution $\mathbf{z}^*$ in the admissible set $\Lambda = \{\mathbf{z} : \mathbf{z} \in BV(\Omega), 0 \leq \mathbf{z} \leq 1\}$.

Proof: (5).

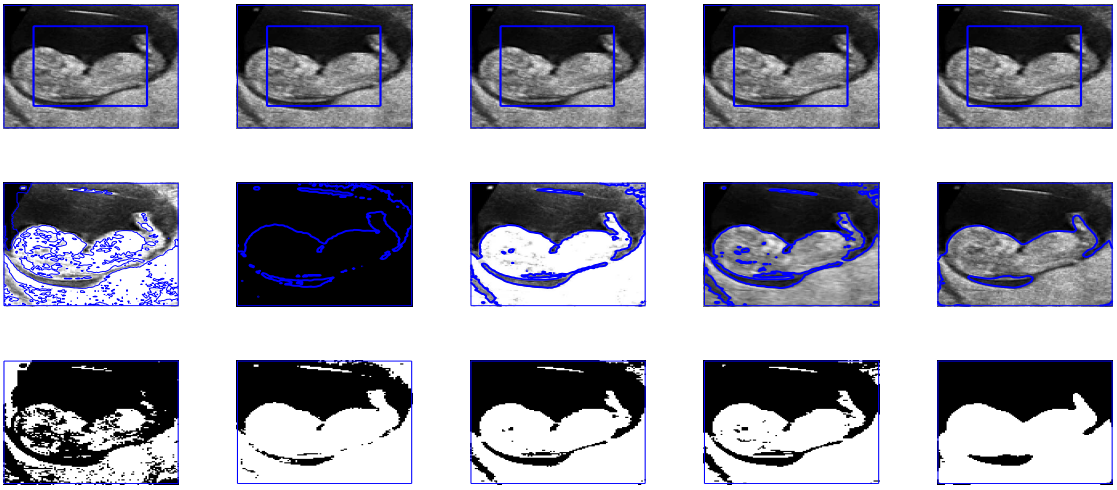

Figure 5. First, second, third and fourth coulumns are the segmentation results of Wu *et al.*[24], Li *et al.*[15], Wu *et al.*[12] and Krinidis *et al.*[31], respectively. Fifth coulumn is the segmentation result of proposed model with $p = 0.6$, μ=0.7, and σ=3.

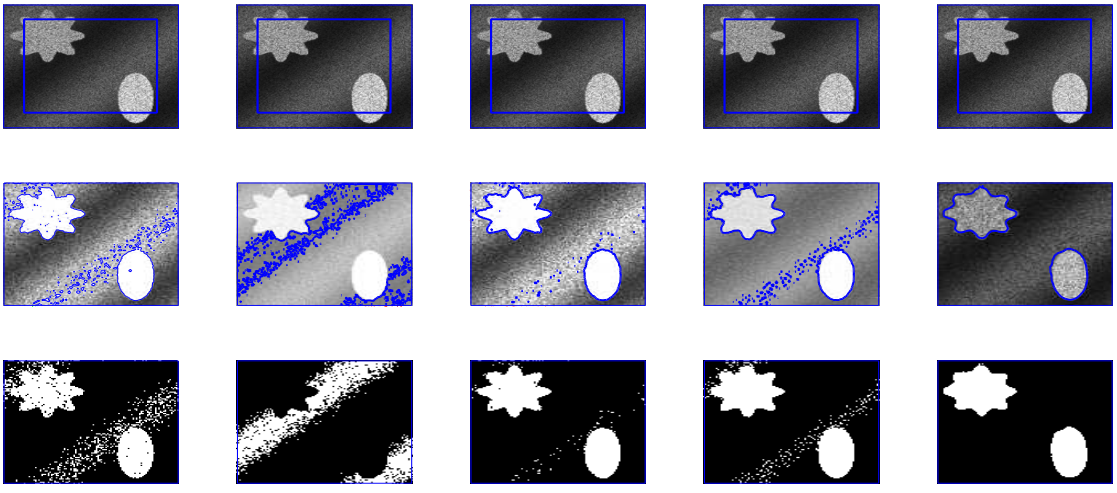

Figure 6. First, second, third and fourth coulumns are the segmentation results of Wu *et al.*[24], Li-kim[15], Wu *et al.*[12] and Krinidis *et al.*[31] respectively. Fifth coulumn is the segmentation result of proposed model with $p = 0.5$, μ=0.7, and σ=3.

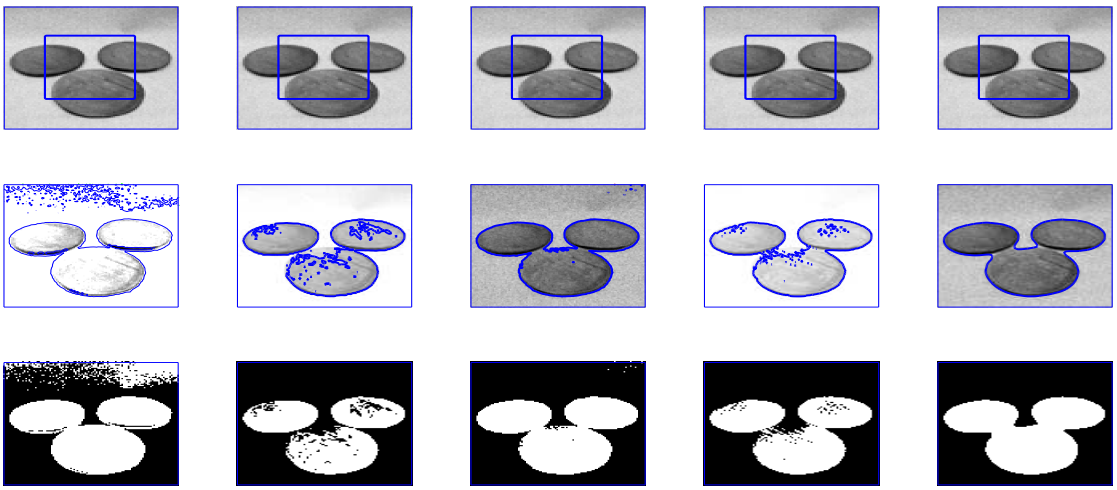

Figure 7. First, second, third and fourth coulumns are the segmentation results of Wu *et al.*[24], Li *et al.*[15], Wu *et al.*[12] and Krinidis *et al.*[31] respectively. Fifth coulumn is the segmentation result of proposed model with $p = 0.5$, μ=0.7, σ=3, and speckle noise = 0.2.

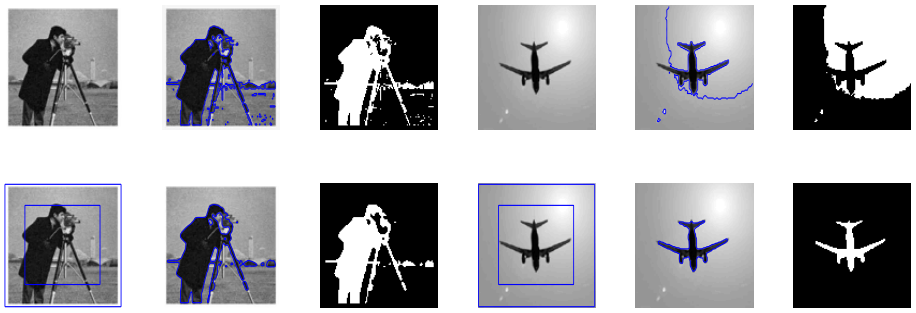

Figure 8. These two inhomogeneous images are taken from Goldstein *et al.*[37]: As Bregman-split method is well known for its speed. But it can be seen that the performence of our proposed model is better than Goldstein *et al.*[37]. The first row is the segmentation result of Goldstein *et al.*[37] and second row is the segmentation result of our proposed model with $p = 0.5$, μ=0.7, and σ=0.6.

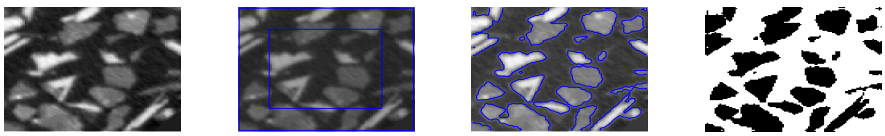

(a) (b) (c) (d)

Figure 9. The segmentation results of the proposed model for the image taken from Furat *et al.*[39]: (a) 2D cut-out of tomographic image data of ore particles, (b) Initial contour, (c) Final contour and (d) Segmentated result of our proposed model with $p = 0.6$, μ=3, and σ=0.5.

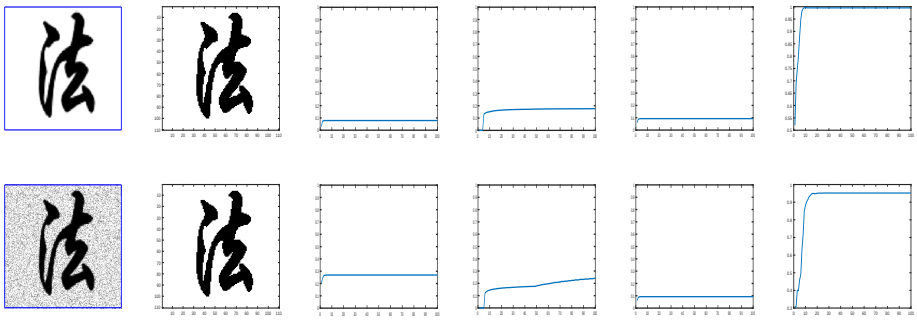

Figure 10. First row image clear image, second row nosy image. Second column shows the clean image. Jaccard similarity coefficient for Wu *et al.*[24], Li *et al.*[15], Krinidis *et al.*[31] and the proposed model with $p = 0.5$,μ=0.7, and σ=3 is shown in the third, forth, fifth and sixth column. x-axis denote the iterations and y-axis is the Jaccard accuracy in each time step iteration.

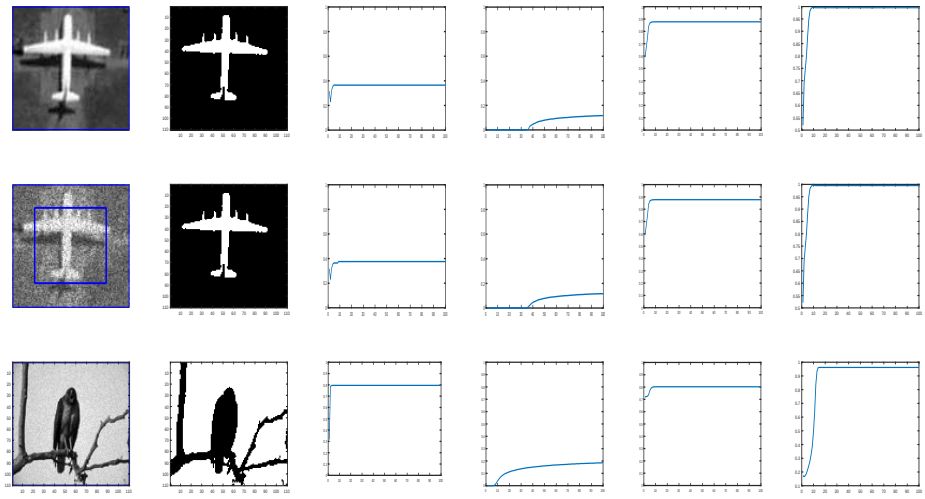

Figure 11. First row a clear image, second row nosy image, and third row is an is taken from Berkeley's data set. Second column shows the clean image. Jaccard similarity coefficient for Wu *et al.*[24], Li *et al.*[15], Krinidis *et al.*[31] and the proposed model with $p = 0.5$, $\mu = 0.7$, and σ=3 is shown in the third, forth, fifth and sixth column. x-axis denote the iterations and y-axis is the Jaccard accuracy in each time step iteration.

4 Experimental results

In this section, we present experiments for real and synthetic image compare the performance of our method to other existing models such as Wu *et al.*[24], Krinidis *et al.*[31], Li *et al.*[15], and Wu *et al.*[12]. The images used in our experiments are of a wide range including medical and real-world images having different sizes and different noise level. The proposed model is also tested for images with intensity inhomogeneity and compared with Goldstein *et al.*[37]. Moreover, different initial guesses have been applied to show the proposed model does not depend on the initialisation and stuck in local minima. In our experiments the parameters $\mu = 0.7$, $p = 0.5$ ()or $p = 0.6$) has been fixed through the experiments. Through experiments we observed that for the parameter p in the range $0.5 \leq p \leq 0.9$ the new model works pretty good. All the experiments were performed on a 1.61 GHz Core $m3-7y30$ CPU @1.00 GHz with 8 GB memory. The algorithm was implemented and carried out using Matlab 9.4, in Windows 10 environment. The image size varies from 100×100 to 256×256.

Test Set 1: Global minima achievement of the new model.

To show the global minima achievement of the proposed model due to its convexity property we run experiments with diferent initialization. Fig. 1 consist of two images (noisy image with three objects and first-ever black hole image) with different initial guess as shown in the first row. As clearly the proposed model does not depend on the initial guesses to archive the same segmentation results. This indicates that the method is independent on the initialization and that there is no need need to check several times for different initial points.

Test Set 2: Robustness and accuracy of the new model

This test set consist of showing the successful performance of the proposed model on noisy images with a single and multiple objects in comparison with well-known models, such as Wu *et al.*[24], Krinidis *et al.*[31], Li *et al.*[15], and Wu *et al.*[12]. Fig. 2 (Berkeley's data set) and 3 are images in presence of high noise and outlier, Fig. 4 and Fig. 5 are medical images, and Fig. 6 and Fig. 7 are noisy images with multi-objects. From all this experiments it can be observed that Wu *et al.*[24], Krinidis *et al.*[31], Li *et al.*[15], and Wu *et al.*[12] fail or partially fail to properly segment the objects in the given images whereas the the proposed method gives satisfactory results.

Test Set 3: Comparison of the proposed model on images with intensity inhomogeneity

Fig. 8 shows the comparison of the proposed model and Goldstein *et al.*[37]. The images with intensity inhomogeneity are also taken from Goldstein *et al.*[37]. It can be observed that the proposed method gives satisfactory results as compare to Goldstein *et al.*[37]. Similarly, Fig. 9 offers a comparison of obtained results using the proposed approach and the model demonstrated in[39]. Note that, the image were taken from Furat *et al.*[39].

Test Set 4: Accuracy analysis thrugh Jaccard similarity coefficient.

We evaluate the accuracy of the proposed model using the Jaccard similarity coefficient. One can quantifying the similarities between the obtained image X and the ground truth Y using the Jaccard index that is mathematically defined by:

$$J(X,Y) = \frac{|X \cap Y|}{|X \cup Y|} \tag{51}$$

In Figs. 10 and 11 we show the quantitative comparison of our proposed model compared to the other existing models such as Wu *et al.*[24], Krinidis *et al.*[31], and Li *et al.*[15] for 5 different images with or without noise. It can be observed that Krinidis *et al.*[31] produced relatively better results compared to Wu *et al.*[24] and Li *et al.*[15], but the results of the proposed model are better than Krinidis *et al.*[31] as clearly seen in the last column of those figures. From the quantitative comparisons, it can be seen that the proposed model performs better than other existing models[15,24,31]. Table 1 shows the JS coefficients comparison of our model with other competing models. The results of this table show 10 images from Berkeley's data set. It can be observed that in terms of accuracy the proposed model is performing better than the competing three other models in almost each image.

Image	proposed model		Krinidis et al.		Wu et al.		Li et al.	
	Iter.	JS	Ite.r	JS	Iter.	JS	Iter.	JS
Img.1	50	0.9999	50	0.9912	300	0.7525	1000	0.2806
Img.2	100	0.8872	100	0.8720	300	0.7747	1000	0.4780
Img.3	100	0.9210	100	0.8890	300	0.4976	800	0.3003
Img.4	100	0.7989	100	0.7922	250	0.7227	1000	0.4043
Img.5	100	0.7210	100	0.6709	300	0.5606	900	0.5437
Img.6	80	0.9194	100	0.5488	300	0.5427	1000	0.3563
Img.7	100	0.7273	100	0.5342	300	0.3440	1000	0.2863
Img.8	100	0.7840	100	0.7839	300	0.7372	1000	0.5321
Img.9	100	0.8458	100	0.8325	300	0.6735	1000	0.3425
Img.10	100	0.8053	100	0.7832	300	0.7452	1000	0.4731

Table 1. Jaccard similarity measure, number of iterations of Krinidis *et al.*, Wu *et al.*, Li *et al.* and of our proposed model on 10 images from Berkeley's data set, image size 110×110.

5 Conclusions and Future Work

This article mainly focuses to design an efficient image data term based on an unconventional and novel objective function - as given by Equation 6. The reason is that this metric is robust against the outliers by giving less weights to outliers and noise in contrast with the conventional and old objective function, given by Equation 2, which give importance to outliers. Besides this a fuzzy level set function is employed with two main benefits over the conventional level set function: capturing more than one phase or objects of different intensities plays an important role while designing a convex functional. In this way, one can impose constraints for convexity, which can be efficiently implemented, avoiding the initial guess tuning. For a deeper understanding of the properties of the proposed model, a mathematical analysis is presented and demonstrated. Moreover, the Gaussian smoothing filtering is employed for the regularization of the fuzzy membership function. Furthermore, for comprehensive analysis of the performance of the proposed model qualitative and quantitative measures are performed on various images. It has been observed that the proposed novel model performs far, and much, better than the existing and latest state-of-the-art segmentation techniques.

Selective image segmentation is one of the most important topics in medical imaging and real applications. In the future, we will work and propose a robust selective segmentation model using a dual-level set variational formulation model that should be based on the local spatial distance. A similar model should aim to segment all objects with one level set function (global) and the selected object with another level set function (local). Furthermore, the combination of marker distance function, edge detection, local spatial distance, and active contour without edges should be considered in the future.

Acknowledgment

The code of the proposed method will be provided for a research purpose if requested from the principal author through email. The work is supported, in parts, by the University of Peshawar and, in parts, by the Abdul wali Khan University, Pakistan.

Appendix

Proof of Theorem 1: Let $\{\mathbf{z}^n\}$ be a minimizing sequence of the energy functional Eq. (31), then there exists a constant M, such that $F(\mathbf{z}^n, c_1, c_2, \alpha, \beta) \leq M$. This implies that

$$\begin{aligned}
&\mu \int_\Omega |\bigtriangledown \mathbf{z}^n(x,y)| dxdy \\
&+ \int_\Omega \alpha(x,y) ||I - c_1||_2^2 [\mathbf{z}^n(x,y)]^m dxdy \\
&+ \int_\Omega \beta(x,y) ||I - c_2||_2^2 [1 - \mathbf{z}^n(x,y)]^m dxdy \leq M. \qquad (52)
\end{aligned}$$

The constraint $0 \leq \mathbf{z} \leq 1$, ensure that $\{\mathbf{z}^n\}$ is uniformly bounded in $BV(\Omega)$. Moreover $BV(\Omega)$ is compact w.r.t $BV_w^*(\Omega)$ topology, then for the subsequence which we also denote by $\{\mathbf{z}^n\}$, $\exists\ \{\mathbf{z}^*\} \in BV(\Omega)$ such that $\mathbf{z}^n \xrightarrow{L^1(\Omega)} \mathbf{z}^*$ and $\mathbf{z}^n \to \mathbf{z}^*$ a.e $x \in \Omega$ and by convergence result the constraint $0 \leq \mathbf{z}^* \leq 1$ also holds. Since $\mathbf{z}^n \to \mathbf{z}^*$ implies that $[\mathbf{z}^n]^m \to [\mathbf{z}^*]^m$ and this implies that $\alpha||\mathbf{u} - c_1||_2^2[\mathbf{z}^n]^m \to \alpha||\mathbf{u} - c_1||_2^2[\mathbf{z}^*]^m$. By Fatou's lemma,

$$\int_\Omega \alpha(\zeta)||\mathbf{u} - c_1||_2^2[\mathbf{z}^*(\zeta)]^m d\zeta \leq \liminf_{n\to\infty} \int_\Omega \alpha(\zeta)||\mathbf{u} - c_1||_2^2[\mathbf{z}^n(\zeta)]^m d\zeta \tag{53}$$

similarly we can write

$$\int_\Omega \beta(\zeta)||\mathbf{u} - c_2||_2^2[1 - \mathbf{z}^*(\zeta)]^m d\zeta \leq \liminf_{n\to\infty} \int_\Omega \beta(\zeta)||\mathbf{u} - c_2||_2^2[1 - \mathbf{z}^n(\zeta)]^m d\zeta \tag{54}$$

also by lower semi-continuity of total variation, we have

$$\int_\Omega |\nabla \mathbf{z}^*(\zeta)| d\zeta \leq \liminf_{n\to\infty} \int_\Omega |\mathbf{z}^n(\zeta)| d\zeta. \tag{55}$$

From Eqs. (41), (42) and (47), we have

$$F(\mathbf{z}^*, c_1, c_2, \alpha, \beta) \leq \liminf_{n\to\infty} F(\mathbf{z}^n, c_1, c_2, \alpha, \beta) \tag{56}$$

thus $\mathbf{z}^* \in \Lambda$ (this complete the proof).
Therefore the minimizer of our proposed model has a global minima.

References

1. D. Mumford, J. Shah, "Optimal approximations by piecewise smooth functions and associated variational problems," *Commun. Pure Appl. Math.*, vol. 42, no. 5, pp. 577-685, Jul. 1989.
2. V. Caselles, R. Kimmel, G. Sapiro, "Geodesic active contours," *Int. J. Comput. Vis.*, vol. 22, no. 1, pp. 61-79, Feb. 1997.
3. C. Li, L. Liu, X. Sun, J. Zhao, J. Yin, "Image segmentation based on fuzzy clustering with cellular automata and features weighting," *EURASIP J.Image Vide.*, vol. 1, pp. 1-11, Dec. 2019.
4. M. Kass, A. Witkin, D. Terzopoulos, "Snakes: Active contour models," *Int. J. Comput. Vis.*, vol. 1, no. 4, pp. 321-331, Jan. 1988.
5. S. Osher, J. A. Sethian, "Fronts propagating with curvature-dependent speed: algorithms based on Hamilton-Jacobi formulations," *J. Comput. Phys.*, vol. 79, no. 1, pp. 12-49, Nov. 1988.
6. S. Pare, A. Kumar, G. K. Singh, V. Bajaj, "Image Segmentation Using Multilevel Thresholding: A Research Review," *Iran. J. Sci. Technol. Trans. Electr. Eng.*, vol. 44, pp. 1-29, Mar. 2020.
7. B. Appleton, H. Talbot, "Globally optimal geodesic active contours," *J. Math. Imaging. Vis.*, vol. 23, no. 1, pp. 67-86, Jul. 2005.
8. A. Yezzi, S. Kichenassamy, A. Kumar, P. Olver, A. Tannenbaum, "A geometric snake model for segmentation of medical imagery," *IEEE Trans. med. imaging.*, vol. 16, no. 2, pp. 199-209, Apr. 1997.
9. T. F. Chan, L. A. Vese, "Active contours without edges," *IEEE Trans. Image Process.*, vol. 10, no. 2, pp. 266-277, Feb. 2001.
10. T. F. Chan, S. Esedoglu, M. Nikolova, "Algorithms for finding global minimizers of image segmentation and denoising models," *SIAM j. Appl. math.*, vol. 66, no. 5, pp. 1632-1648, 2006.
11. L. D. Cohen, "On active contour models and balloons," *CVGIP: Image Und.*, vol. 53, no. 2, pp. 211-218, Mar. 1991.
12. Y. Wu, W. Ma, M. Gong, H. Li, L. Jiao, "Novel fuzzy active contour model with kernel metric for image segmentation," *Appl. Soft Comput.*, vol. 34, pp. 301-311, Sep. 2015.

13. J. Lie, M. Lysaker, X. C. Tai, "A binary level set model and some applications for Mumford *et al.* image segmentation," *IEEE Trans. Image Process*., vol. 15, no. 4, pp. 1171-1181, Apr. 2006.

14. K. Zhang, L. Zhang, H. Song, W. Zhou, "Active contours with selective local or global segmentation: a new formulation and level set method," *Image. Vision. comput*., vol. 28, no. 4, pp. 668-676, Apr. 2010.

15. Y. Li, J. Kim, "An unconditionally stable numerical method for bimodal image segmentation," *Appl. Math. Comput*., vol. 219, no. 6, pp. 3083-3090, Nov. 2012.

16. A. Mondal, S. Ghosh, A. Ghosh, "Robust global and local fuzzy energy based active contour for image segmentation," *Appl. Soft Comput*., vol. 47, pp. 191-215, Oct. 2016.

17. C. Wang and B. Zhu, "Image Segmentation and Adaptive Contrast Enhancement for Haze Removal," *IEEE 63rd International Midwest Symposium on Circuits and Systems (MWSCAS)*., pp. 1036-1039, 2020, doi: 10.1109/MWSCAS48704.2020.9184525.

18. A. Joshi, M. S. Khan, S. Soomro, A. Niaz, B. S. Han and K. N. Choi, "SRIS: Saliency-Based Region Detection and Image Segmentation of COVID-19 Infected Cases," *IEEE Access*., vol. 8, pp. 190487-190503, 2020, doi: 10.1109/ACCESS.2020.3032288.

19. K. S. Chuang, H. L. Tzeng, S. Chen, J.Wu, T. J. Chen, "Fuzzy c-means clustering with spatial information for image segmentation," *computerized medical imaging and graphics*., vol. 30, no. (1) pp. 9-15, Jan. 2006.

20. B. K. Tripathy, A. Basu, S. Govel, "Image segmentation using spatial intuitionistic fuzzy C means clustering," *IEEE International Conference on Computational Intelligence and Computing Research*., pp. 1-5, Dec. 2014.

21. Y. Chen, H. D. Tagare, S. Thiruvenkadam, F. Huang, D. Wilson, K. S. Gopinath, E. A. Geiser, "Using prior shapes in geometric active contours in a variational framework," *Int. J. Comput. Vis*., vol. 50, no. 3, pp. 315-328, Dec. 2002.

22. H. Ali, N. Shah, K. Chen, G. A. Khan, "A variational model with hybrid images data fitting energies for segmentation of images with intensity inhomogeneity," *Pattern Recognit*., vol. 51, pp. 27-42, Mar. 2016.

23. C. Li, C. Xu, C. Gui, M. D. Fox, "Level set evolution without re-initialization: a new variational formulation," *Proc. IEEE Conf. Comput. Vis. Pattern Recognit*., vol. 1, pp. 430-436, Jun. 2005.

24. Y. Wu, C. He, "A convex variational level set model for image segmentation," *Signal Process*., vol. 106, pp. 123-133, Jan. 2015.

25. L. I. Rudin, S. Osher, E. Fatemi, "Nonlinear total variation based noise removal algorithms," *Physica D: nonlinear phenomena*., vol. 60, no. 1-4, pp. 259-268, Nov. 1992.

26. N. Badshah, K. Chen2, H. Ali and G. Murtaza. Coefficient of Variation Based Image Selective Segmentation Model Using Active Contours. *East Asian Journal on Applied Mathematics*., vol. 2, no. 2, pp. 150-169, May 2012. doi: 10.4208/eajam.090312.190412a.

27. Y. Yu, S. T. Acton, "Edge Detection in Ultrasound Imagery Using the Instantaneous Coefficient of Variation," *IEEE Trans. Image Process*., vol. 13, no. 12, pp. 1640 - 1655J, Jan 2005. DOI: 10.1109/TIP.2004.836166.

28. H. Ali, N. Shah, K. Chen, G. A. Khan, N. Zikria, "Multiphase segmentation based on new signed pressure force functions and one level set function," *Turk. J. Electr. Eng. Co*., vol. 25, no. 4, pp. 2943-2955, Jul. 2017.

29. J. Oh, N. Kwak, "Generalized mean for robust principal component analysis," *Pattern Recognit*., vol. 54, pp. 116-127, Jun. 2016.

30. S. Balla-Arabé, X. Gao, B. Wang, "A fast and robust level set method for image segmentation using fuzzy clustering and lattice Boltzmann method," *IEEE T. Cybernetics*., vol. 43, no. 3, pp. 910-920, Mar. 2013.

31. S. Krinidis, V. Chatzis, "Fuzzy energy-based active contours," *IEEE Trans. Image Process*., vol. 18, no. 12, pp. 2747-2755, Aug. 2009.

32. B. Song, T. Chan, "A fast algorithm for level set based optimization," *UCLA CamReport*., vol. 2, pp. 68, Dec. 2002.

33. S. H. Lee, J. K. Seo, "Level set-based bimodal segmentation with stationary global minimum," *IEEE Trans. Image Process*., vol. 15, no. 9, pp. 2843-2852, Aug. 2006.

34. H. Ali, A. Shujjahuddin, L. Rada, "A New Active Contours Image Segmentation Model Driven by Generalized Mean with Outlier Restoration Achievements" *International J. of Pattern Recognit and Artificial Intelligence*., 2019. DOI: 10.1142/S0218001420540269.

35. M. Gong, Y. Liang, J. Shi, W. Ma, J. Ma, "Fuzzy c-means clustering with local information and kernel metric for image segmentation," *IEEE Trans. Image Process*., vol. 22, no. 2, pp. 573-584, Sep. 2013.

36. X. Cai, "Variational image segmentation model coupled with image restoration achievements," *Pattern Recognit*., vol. 48, no. 6, pp. 2029-2042, Jun. 2015.

37. T. Goldstein, X. Bresson, S. Osher, "Geometric applications of the split Bregman method: segmentation and surface reconstruction," *J. Sci. Comput*., vol. 45, no. 1-3, pp. 272-93, Oct. 2010.

38. C. Li, C. Y. Kao, J. C. Gore, Z. Ding, "Implicit active contours driven by local binary fitting energy," *in proc. IEEE Conf. Comput. Vis. Pattern Recognit. (CVPR).,* vol. 42, pp. 1-7, Jun. 2007.

39. O. Furat, M. Wang, M. Neumann, L. Petrich, M. Weber, C. E. Krill III, V. Schmidt, "Machine learning techniques for the segmentation of tomographic image data of functional materials," *Frontiers in Materials.,* vol. 6, pp. 145, Jun. 2019.